LIMNOLOGY and OCEANOGRAPHY

ASLO

Limnol. Oceanogr. 9999, 2023, 1–12

doi: 10.1002/lno.12332

Temporal dynamics of heatwaves are key drivers of sediment mixing by bioturbators

Zhengquan Zhou,[1,2*] **Natalie Steiner**,[1] **Gregory S. Fivash**,[1] **Francesco Cozzoli**,[3,4,5] **Daniel B. Blok**,[1] **Lennart van IJzerloo**,[1,2] **Jeroen van Dalen**,[1] **Tom Ysebaert**,[1,6] **Brenda Walles**,[6] **Tjeerd J. Bouma**[1,2,7]

[1]NIOZ Royal Netherlands Institute for Sea Research, Department of Estuarine and Delta Systems, Utrecht University, Yerseke, The Netherlands
[2]Faculty of Geosciences, Department of Physical Geography, Utrecht University, The Netherlands
[3]Research Institute on Terrestrial Ecosystems (IRET-URT Lecce), National Research Council of Italy (CNR), Campus Ecotekne, Lecce, Italy
[4]National Biodiversity Future Center, Palermo, Italy
[5]Laboratory of Ecology, Department of Biological and Environmental Sciences and Technologies, University of Salento, Lecce, Italy
[6]Wageningen Marine Research, Wageningen University and Research, Yerseke, The Netherlands
[7]University of Applied Sciences, Vlissingen, The Netherlands

Abstract

Heatwaves affect tidal flat ecosystems by altering the bioturbating behavior of benthic species, with potential consequences for sediment oxygenation, particle mixing, and erodibility. Although the frequency and duration of heatwaves are expected to increase under global warming scenarios, we lack insights into how heatwaves' temporal dynamics affect bioturbating behaviors. Using the widely distributed bioturbator *Cerastoderma edule* as model species, we quantified how heatwaves with identical heat-sum but different temporal dynamics (i.e., 3- vs. 6-d heating and normal temperature cycles) affect bioturbating behaviors and the sediment mixing processes in tidal mesocosms. Our results show that short but frequent 3-d heatwave cycles increased the magnitude of bioturbating behaviors, thereby resulting in more bio-mixed sediment than observed under infrequent prolonged 6-d heatwave cycles. This unexpected result could be ascribed to the weakening health condition indicated by a high death rate (47.37%) under 6-d heatwave cycles than in 3-d and no-heatwave control cycles. Present findings reveal that the impact of heatwaves on sediment bioturbation will strongly depend on the temporal dynamics of future heatwaves: bioturbation will be enhanced unless the heatwave duration exceeds species resistance and increases mortality.

*Correspondence: zhengquan.zhou@nioz.nl

Additional Supporting Information may be found in the online version of this article.

Author Contribution Statement: Z.Z.: Conceptualization, investigation, methodology, data curation and analysis, visualization, writing—original draft. N.S.: Conceptualization, investigation, methodology, data curation and analysis, writing review and editing. G.S.F.: Statistics, data curation, visualization, writing review and editing. F.C.: Conceptualization, visualization. D.B.B.: Investigation, methodology, mesocosm realization, sample collection. L.I.: Investigation, data curation, software, methodology. J.D.: Investigation, methodology, mesocosm realization. T.Y.: Conceptualization, investigation, methodology. B.W.: Conceptualization, investigation, methodology, writing review and editing. T.J.B.: Conceptualization, methodology, visualization, writing review and editing, funding acquisition, project administration.

Bioturbation is the process of sediment reworking by living organisms (Darwin 1881). Bioturbators are classified as ecosystem engineers (Jones et al. 1997; Wright and Jones 2006) because they can excessively modify the physical properties of sediments (e.g., compaction, bulk density, and particle distribution) and the diffusion rate of chemical compounds (Braeckman et al. 2010; Kristensen et al. 2012; Cozzoli et al. 2021) via foraging (Wrede et al. 2018) and building behaviors (Borsje et al. 2014). From terrestrial fields to deep-sea sediments, bioturbation plays a significant role in changing the surface landscape of our planet (Meysman et al. 2006). Across the globe, tidal flats are one of the most renowned ecosystems dominated by a wide range of bioturbating benthic species (Teal et al. 2008; van der Wal et al. 2017), and hence the focus of the present study.

The physical conditions for living on tidal flats are typically harsh in that they constantly change due to tidal cycles of drying and inundation. By interacting with physical forces from

currents and waves, some bioturbators actively flush their burrows to refill oxygen and nutrients (Mermillod-Blondin and Rosenberg 2006; Hedman et al. 2011). These burrows thus become networks to promote chemical exchange at water-sediment interfaces (i.e., benthic–pelagic coupling). Moreover, bioturbators loosen the sediment and increase the surface roughness (Widdows and Brinsley 2002; Li et al. 2017). Hydrodynamic forces may reshape these biologically induced topographies during tidal inundation, resulting in enhanced sediment resuspension and erosion (Montserrat et al. 2009; Cozzoli et al. 2019; Dairain et al. 2020). For example, the common cockle *Cerestoderma edule* can affect sediment stability through vertical and horizontal movements such as shell shaking, adductions, and excreting feces. These bioturbating activities can lead to more erosion in cohesive sediment (Widdows et al. 2000; Le Hir et al. 2007; Li et al. 2017). Understanding the effect of benthic bioturbators on sediment erodibility is essential, as short-term transitions between erosion and accretion may affect the long-term stability of tidal flat ecosystems (e.g., *see* Bouma et al. 2016; Shi et al. 2021).

Tidal flat ecosystems worldwide are declining and may be increasingly threatened by global change processes (Murray et al. 2019). Recent studies show that 50% of the ocean surface water may suffer from marine heatwaves by the late 21st century (Holbrook et al. 2019). Tidal flat ecosystems are expected to be much more prone to such heatwaves since the surface sediments can experience a daily temperature difference of more than 10°C during the low-tide emersion time (Johnson 1965; Bouchet et al. 2007; Li et al. 2019), despite that the seasonal variation can be more than 30°C from summer to winter (Murphy and Reidenbach 2016). Goulletquer et al. (1998) even measure a daily temperature increment of 23°C in the oyster reef. Bioturbators living on tidal flats are prone to extreme temperature fluctuations, particularly those inhabiting higher intertidal areas (Pansch et al. 2018). Occasional exposure to heatwaves can decrease the health conditions of the benthic bioturbators living on tidal flats (Coma et al. 2009; Pairaud et al. 2014; Rivetti et al. 2014). Thermal stress typically promotes the bioturbators' metabolic rates (Anestis et al. 2007; Vinagre et al. 2016), which positively relates to their moving behavior (Cozzoli et al. 2019). More movements may increase sediment bio-mixing and a reduced critical erosion threshold on the tidal flat scale (Cozzoli et al. 2020). Thus, to predict the future fate of tidal flat ecosystems, it is necessary to better understand how future heatwaves affect benthos' bioturbation behaviors.

Like most abiotic stresses and disturbances in the natural environment, the effect of heatwaves may be expected to depend on their magnitude, duration, and frequency (Donohue et al. 2016). To date, most heatwave studies only focus on magnitude (i.e., the effects of the heatwave intensity; Perkins-Kirkpatrick et al. 2017; Gauzens et al. 2020; Laufkötter et al. 2020), even though variation in duration and frequency may impose more complex outcomes. For example, Seuront et al. (2019) show that 100% mortality for the mussel *Mytilus edulis* occurred at lower temperatures with increasing duration of exposure to heatwaves. Global warming not only leads to a higher heatwave intensity, but also amplifies the temporal dynamics of heatwaves. That is, the duration and frequency of marine heatwaves have increased by 17% and 34%, respectively, in the years 1987–2016 compared to the years 1925–1954 (Oliver et al. 2018). Thus, in addition to experiments quantifying the effects of heatwave intensity on bioturbation behavior and changes in tidal flat sediments, studies are needed to quantify the impact of temporal dynamics.

To gain insights into the effects of heatwave temporal dynamics on the bioturbation process, we conducted a mesocosm experiment with contrasting "short" and "long" heatwave cycles. Both cycles consist of 12-d heating and 12-d recovery phases, while the temporal distribution of heating and recovery treatments are different: the "short-duration" heatwaves consist of alternating 3-d heating and normal temperature periods; the "long-duration" heatwaves consist of alternating 6-d heating and normal temperature periods (Fig. 1). The control treatment is kept constantly under ambient temperatures of 20°C. The heatwave temperature was 35°C during daytime low tides. In each mesocosm, a regular semidiurnal tide was mimicked with a 5-h low tide during the day and 5 h at night. We used the widely distributed common cockle *C. edule* as a model bioturbator species. Cockles' burrowing depth, sediment mixing, and survival were measured to study the bioturbation response patterns under different heatwave profiles.

Material and methods

Mesocosm setups

A mesocosm experiment was performed in a climate room to simulate natural heatwaves on tidal flats. One tidal mesocosm unit consists of two water tanks stacked together (inner dimensions: 110 × 95 × 60 cm). The upper tank was filled with 30-cm-high sand (SD50 = 265.02 μm) as a basement that contained the experimental treatments; the lower tank was used as a water reservoir for simulations of tidal cycles (for details, *see* Zhou et al. 2022). The experimental treatments created a high tide by pumping water from the lower reservoir tank into the upper tank. The water height was adjusted by a return-flow pipe (30 cm height), transporting the overflow water back to the lower tank. Low tide was created by turning off the pump to drain all water into the lower reservoir tank. A regular semidiurnal tide was mimicked according to the natural conditions where cockles were collected (Oesterdam, 51°28′01.4″N, 4°12′49.8″E). The low tide period was 5 h occurring twice daily during both day and night, giving a total of 10 h low tide per day (Fig. 1a).

PVC pots (67 mm inner diameter, 3 mm wall thickness, 100 mm height) were filled with sieved sediment (mesh size Ø = 1000 μm, sediment SD50 = 158 μm) and placed in the

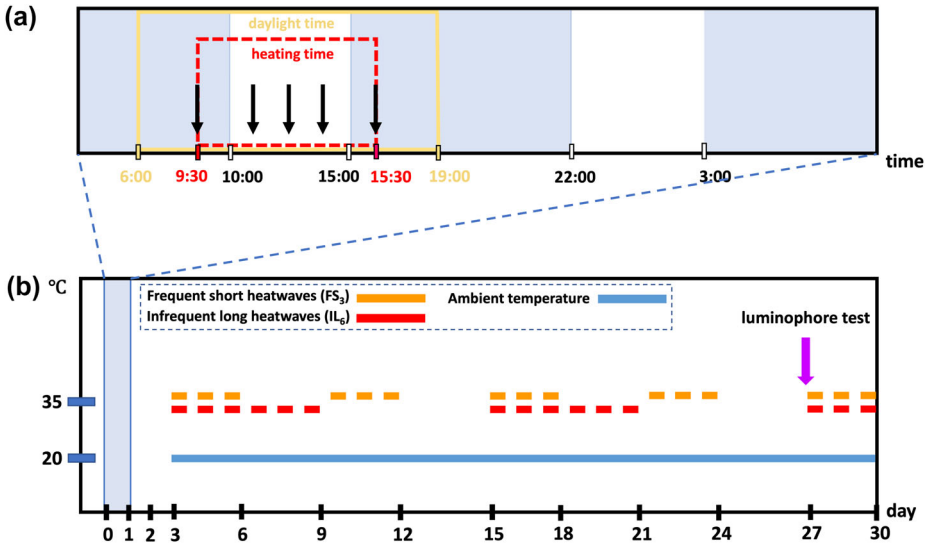

Fig. 1. Schematic representation of the daily tidal regime (**a**) and simulated heatwave treatments (**b**). In the daily tidal regime (**a**), daylight time is indicated by a yellow color on the time axis. In contrast, nighttime is marked as black. Semidiurnal tides (42% low tide time) were mimicked (i.e., high tide marked as blue shades, low tide marked as white rectangles). In panel (**a**), the times at which burrowing depth measurements were taken are indicated by black arrows. The ambient air temperature was constant at 20°C (**b**, indicated by the solid blue line). The heaters were only turned on during the daytime low-tide period, as indicated by the dashed lines starting half an hour before and ending half an hour after low-tide (**a**, the red frame). The maximal temperature of the simulated heatwave was 35°C. Two heatwave temporal profiles were applied, a frequent short-duration heatwave (**b**, 3-d cycles) and a less frequent long-duration heatwave (**b**, 6-d cycles). Both heatwaves followed a 3-d heatwave to measure bioturbation effects using luminophores. The purple arrows indicate when luminophore tablets are deployed during the low tides.

upper mesocosm tanks for holding the cockles to be used in the experiment. These pots were made by cutting long 5000 mm PVC pipes into a shorter uniform size, then adding ventilated bottom covers at one end. There are three types of experimental pots: (1) "heatwave" pots with cockles inside that experienced a 3-d cycle or the 6-d cycle heatwaves (FS_3 and IL_6; details in next section), (2) "control" pots with cockles inside and were under ambient temperatures, and (3) "blank" pots that contained no cockles under ambient temperature, to only measure the tidal effects on sediment mixing. There were 40 "heatwave" pots; 20 replicates for each heatwave profile. The "control" pots had 20 replicates, and the "blank" pots had 10 replicates. All pots were evenly distributed in four mesocosms, two with heaters on top and two without under ambient temperature.

Imposing heatwaves: Temperature setting and measurement

Four mesocosms were placed in the same climate room, of which two were used for simulated heatwave treatments and the other two as ambient temperature controls. According to temperature measurements in the field during the 2020 summertime heatwaves (*see* Supporting Information Appendix S1, Fig. SA1a), we set the maximal temperature of the sediment surface at 35°C and the ambient temperature at a constant 20°C. Terrace heaters (Frico, EZ212) were used to mimic solar irradiation during low tide. A thermal probe was placed on top of the sediment to control the heater temperature by real-time measurements: when the temperature of the sediment surface reached 35°C, the heater was turned off; when it dropped below 35°C, it was turned on again.

Due to delays in the control system, the actual mean temperature was 32.23 ± 1.61°C (*see* Supporting Information Appendix S1, Fig. SA1b, red lines); the actual mean ambient temperature was 16.42 ± 0.35°C (Fig. SA1b, blue lines). The daily operating time of the heater was controlled by a time switch to match the daytime low tide period, starting to heat half an hour before the daytime low tide till half an hour after the daytime low tide (Fig. 1a). The heaters were turned off during the night.

To measure the temperature profiles in each tank, two extra PVC pots (no cockles inside) were made to hold the temperature sensors (PT-100 sensors, TC Direct). These sensors were deployed at fixed depths of 0, 3, and 6 cm to record the per-minute temperature profiles in the PVC pots, and they were used to represent the temperature profiles of all pots in the same tank. All temperature sensors were connected to a CR10X datalogger (Campbell Scientific Inc.), and the data was transferred via LoggerNet software (Campbell Scientific Inc.). During low tides, the temperature sensors measured the temperature of drained sediment in PVC pots; during high tides, all sensors were submerged and measured water temperature instead.

To determine a reasonable magnitude and duration for the artificial heatwaves in our experiment, we obtained 70 yr of temperature data from the Royal Netherlands Meteorological

Institute (KNMI) at Schiphol (near Amsterdam), Netherlands. The "high-temperature event" was summarized as when the daily maximum temperature was above 30°C for more than 2 d. In the past 70 yr, there were 42 high-temperature events lasting more than 2 d, 35 of which lasted 2–3 d, 5 of which lasted for 4–5 d, and 2 of which lasted more than 6 d (*see* Supporting Information Appendix S2, Table S1). Therefore, two heating treatments were applied to mimic: (1) frequent short-duration (i.e., FS_3) heatwaves consisting of four repeating cycles of 3-d heating within between 3-d recovery at normal temperatures; (2) infrequent long-duration (i.e., IL_6) heatwaves consisting of two repeating cycles of 6-d heating within between 6-d recovery at normal temperatures (Fig. 1b). The overall heatwave exposure had an identical duration for FS_3 and IL_6 during the day, with 5 h per day for 12 d. The FS_3 and IL_6 heatwave treatments ended with a 3-d heatwave to measure bioturbation using luminophores (*see* Quantifying the sediment mixing process using luminophores). The ambient control was maintained at a constant temperature of 20°C over the whole period.

C. edule as model species to study bioturbation

The common cockle *C. edule* is widely distributed along the European Atlantic coastline. The cockles used in this experiment were collected from Oesterdam, the Netherlands, in late September 2020. They were transported to a temperature-controlled climate room set at 20°C and left in a tank filled with aerated seawater for 120 h acclimation. Then, living cockles were transferred into PVC pots filled with sediment and placed in the tidal mesocosms, allowing them to acclimate to the new environment for another 72 h before starting the heatwave treatments. Each PVC pot under FS_3, IL_6, and the control treatment received one live cockle taken from a population with a mean shell length of 32.00 ± 1.80 mm and a mean wet tissue weight of 0.91 ± 0.21 g (mean ± SD; $n = 50$). When individuals were inactive or remained on the sediment surface for 24 h, they were replaced with new individuals. All cockles were fed twice a week with instant microalgae (Shellfish Diet 1800; Reed Mariculture Inc.). The algae concentrate was prediluted at 10 : 1 with 100 mL seawater, then fed to each tank homogeneously with a dropper. One-third of the seawater in the reservoir tanks was replaced every week to guarantee good water quality throughout the experiment. Dead cockles on the sediment surface were removed every day. We used a metal tweezer gently moving around their siphons to check whether cockles had died and burrowed in the sediment. Cockles that did not respond to these physical stimuli were recorded as dead.

Burrowing behavior measurements

We use bivalves' burrowing behavior as an indicator of vertical bioturbation activity. A cotton thread was glued (superglue CA10; F.T Products) on the cockle's shell to measure the cockle's burrowing behavior. The other end of the line is tied with a knot to make different measurements comparable for the same cockle. The thread was gently pulled straight to measure the distance between the knot and the sediment surface. This method was adopted from Auffrey et al. (2004) and has been tested to have no effects on the burrowing activities of bivalves. Moreover, we have successfully applied this method to detect the significant impact of heatwaves on the cockles' burrowing behavior (Zhou et al. 2022). Five measurements were performed daily. The first and last measurement occurred half an hour before and after the 5-h low tide at 09:30 h and 16:30 h. The other three measurements occurred during the low tide at 10:30 h, 12:30 h, and 14:30 h, during which the sediment with cockles was directly exposed to solar radiation in the heating mesocosms (Fig. 1a). The relative depth change of each measurement point is calculated by subtracting the first measurement value from the absolute length. Therefore, the relative depth change of the first measurement was always 0 cm at 09:00 h. The following four measurements used the first one as a baseline to calculate the burrowing depth change.

Quantifying the sediment mixing process using luminophores

We used luminophores (Environmental Tracing Systems Ltd.) to quantify sediment particle transportation in each PVC pot. Luminophores are inert natural sediment particles dyed with luminescent paint and are often used to track bioturbation effects (Wiesebron et al. 2021). The median grain size (SD50) of the luminophores was 41 μm. The color of the luminophores was "magenta red" under normal ambient light, with shining luminosity in a dark environment under UV light. Sieved ($Ø = 1000\ \mu$m) ambient sediment (SD50 = 158 μm) and luminophores were mixed at a volume ratio of 10 : 1 with water (i.e., water weight was determined by the bulk density of ambient sediment). Then, the sediment-luminophore-water mixture was poured into PVC molds of $70 \times 70 \times 0.5$ mm (i.e., inner diameter = 67 mm) and froze at −20°C to make luminophore "tablets".

Luminophore tablets were placed on top of each PVC pot during low tide for all treatments, namely, "heatwaves (i.e., FS_3 and IL_6)," "control," and "blank." After this deployment, a final 3-d heatwave treatment was applied to both the FS_3 and IL_6 "heatwave" pots, but not to the no-heatwave "control" and "blank" pots (Fig. 1b). When the experiment ended, the PVC pots with luminophores were horizontally sliced using a metal spade along depth gradients (i.e., every 0.5 cm till 3.0 cm, then 1.0 cm per slice till 5.0 cm). The luminophore area in each slice was used to indicate the horizontal bioturbation activities.

Every slice was photographed under UV light using a digital single-lens reflex camera (Canon EOS with 18–55 mm EFS objective). The camera was mounted on a fixed stand to guarantee the same shooting distance. The JPEG images were saved as 2304×3456 pixels. These images were processed using a

custom script of ImageJ2 and R 4.0.0 software. First, the images were subdivided into RGB stacks, and the brightness threshold of red 128–255 was used to distinguish the image pixels in red luminophores and sediment. Then, the total number of luminophore pixels in each slice was counted ($S_{\text{bioturb-depth}}$, cm^2). Only pixels within the circular region in the center frame of the photo (within the PVC tube) were analyzed. A buffer margin of 5 mm from the edge within the tube was also excluded to minimize edge effects due to the cutting process.

Since luminophores were applied on top of the sediment, the luminophore counts in photographs taken from the top view of below-ground sediment slices provide a quantitative indicator of the bioturbation activity in an individual PVC core. Due to limitations of the slicing tool, in all cores, the first two sediment slices taken at a depth of 0.5 cm and 1 cm were disturbed by edge effects and thus neglected. As < 1% luminophore pixels were observed in slices taken below 3 cm (i.e., at 4 and 5 cm depth), these slices were also neglected. As a result, the luminophore counts in photographs taken from the top of the sediment slices at 1.0, 1.5, 2.0, 2.5, and 3.0 cm were used to calculate the average bioturbation areas with the following equation:

$$S_{\text{bioturb}} = \sum_{i=1}^{n} \left(\frac{PixelsL_i}{PixelsS_i} \times 100\% \times S_{\text{pvc}} \right) / n, \quad (1)$$

where S_{bioturb} is the depth-averaged bioturbated surface area in each PVC core (cm^2); i is the slice number (i.e., five slices in each core); $PixelsL_i$ and $PixelsS_i$ refer to the luminophore pixel amount and the total pixel amounts of sediments in slice i, respectively; S_{PVC} refers to the cross-sectional area of one PVC pots (i.e., 35.24 cm^2); n is the number of layers averaged ($n = 5$ for all cores).

Data analysis

Survival percentage

The number of living cockles during the experimental period was divided by the total number of replicates (excluding replicates lost due to the accident, *see* Supporting Information Appendix S3) to calculate the survival percentage for FS_3, IL_6, and ambient control treatments.

Burrowing depth

The burrowing depth measurement was an indicator of vertical bioturbation activities. A linear mixed-effect model was used to test the effects of heatwave treatments on cockles' burrowing depths: *Burrowing depth change* ~ *Heatwave treatment* + *Day* + (1|*Individual number*). The heatwave treatments and experimental days are fixed factors, while the individual serial number is a random factor nested within the fixed factors. Finally, a post hoc Tukey HSD analysis was applied to check the effects of different heatwave cycles on burrowing depth change.

Luminophore tests

We used luminophore tests to get quantitative proxies for bioturbation activities. That is, we calculated first the depth-specific bioturbation area ($S_{\text{bioturb-depth}}$, cm^2) for each 5-mm slice along a 1- to 3-cm depth profile and used these data to derive the depth-averaged bioturbation area (S_{bioturb}, cm^2) in each PVC core. Since the luminophore tests were only applied once at the end of the experiment, we could not do a time-series analysis.

The effects of heatwave treatments on the depth-specific bioturbation profiles were tested using a two-way analysis of covariance (ANCOVA): *Bioturbation areas* ~ *Heatwave treatment* + *Depth*, followed by a Tukey HSD analysis for post hoc analysis. The effects of heatwave treatments on the depth-averaged bioturbation areas were first checked by the Kruskal–Wallis test, and then a Wilcoxon rank sum test was used as a post hoc analysis.

The data points and error bars indicate mean ± standard error in all plots. The data analysis was performed by R 4.0.0 (R Core Team 2021).

Results

Cockles' response to thermal stress: Mortality and behavior

Repeated exposure to heatwaves (defined as temperatures ≥ 35°C) can lead to the death of cockles. The 3-d cycle heatwaves (FS_3) resulted in a 72.73% survival rate (*see* Supporting Information Appendix S3, Fig. SA2). Even though the total number of heating days was the same, the 6-d cycle heatwaves (IL_6) resulted in a lower survival rate at 47.37% (Fig. SA2). The same applies when comparing the survival rate of IL_6 to the survival rate in the absence of any thermal stress (no-heatwave controls, 100% survival). The method of behavioral measurement can detect significant differences in the burrowing depth under different heatwave settings (significance levels are shown in Fig. 2). The burrowing behavior of cockles was affected by thermal stress (Fig. 2). During low tide, the cockles burrowed deeper into the sediment when exposed to heatwave conditions (Fig. 2b). Upon the return of the high tide, the cockles then moved toward the surface. On ambient temperature days between heatwaves, the behavior of cockles that had earlier experienced heatwaves returned to movement patterns similar to those seen in cockles in the permanently ambient temperature treatments (Fig. 2a).

Bioturbation effects: The area of disturbed sediments

Cockles' activities always introduced the surface particles into up to 3 cm sediment layers, resulting in similar overarching patterns as shown in Fig. 3. The horizontal bioturbation areas differed between treatments: the bioturbating areas under FS_3 were the largest, and those under IL_6 were the smallest. This trend was consistent from 1.0 to 2.5 cm depth (Fig. 3). The statistical results for Fig. 3 are shown in Tables S4, S5 in Supporting Information Appendix S5.

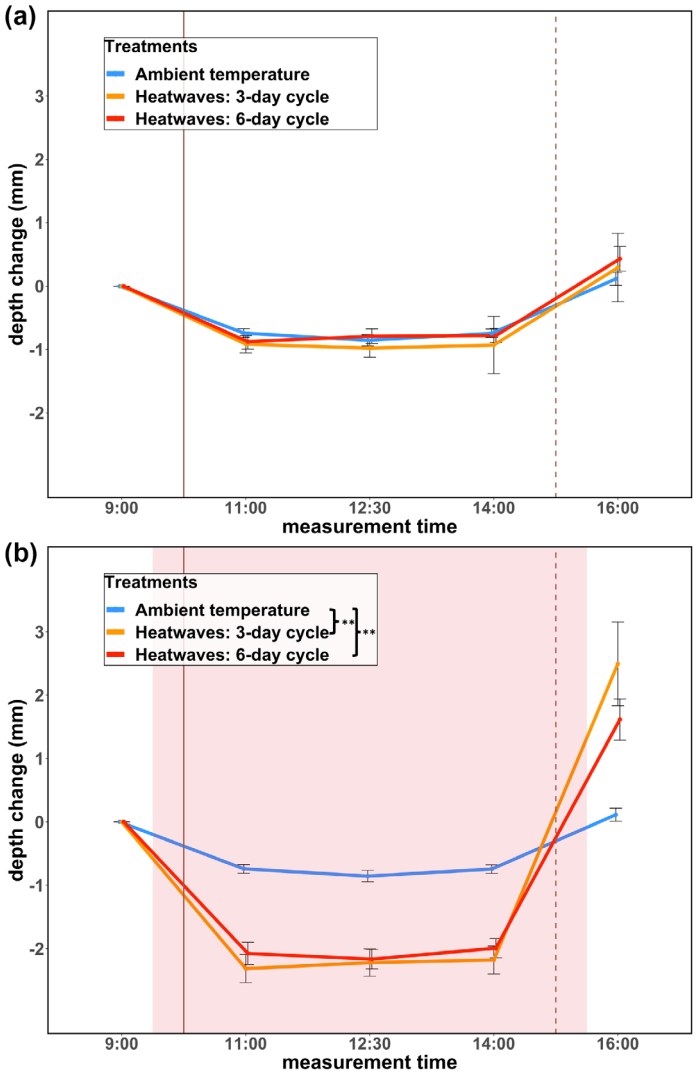

Fig. 2. Daily average burrowing position as measured during the non-heatwave cycles (**a**) and heatwave cycles (**b**). Different line colors indicate temperature settings, as shown in the legends. The red shades represent the period of the heating treatment. The solid brown lines represent the beginning time of low tides (start of sediment exposure); the dashed brown lines represent the beginning time of high tides (start of sediment submersion). Data from individual measurements were averaged daily by each heatwave and recovery cycle. In the plot, each point represents the mean values of the measured alive individuals. The calculation was based on 72–540 recordings in panel (**a**), and 95–540 recordings in panel (**b**), depending on the survival individuals under the control/heatwave treatments. The ambient control measurements (blue lines) in panels (**a**) and (**b**) are identical based on all daily recordings in each heatwave/cycle setting. Positive depth change values indicate cockles move upwards, while negative values indicate moving downwards. The error bars represent the standard errors of individual measurements during all repeated cycles. The difference in depth changes between control and heatwave treatments were tested using one-way ANOVA. The significant level $p < 0.01$ was marked by "**" on the right side of the figure legends.

The heatwave duration significantly impacted the amount of biodisturbed sediments (Table 4, ANCOVA, $F = 12.01$, $df_{treatments} = 2$, $p < 0.01$). Post hoc analysis showed that the 6-d cycle heatwaves (IL_6,) significantly decreased the size of biodisturbed areas compared with that under 3-d cycle heatwaves (FS_3) (Table 5, Tukey HSD, $t = -4.81$, $df_{treatments} = 2$, $df_{depths} = 4$, $p < 0.01$). However, the 3-d cycle heatwaves imposed similar bioturbation effects with those under control ambient temperatures (Table 5, Tukey HSD, $t = 1.82$, $df_{treatments} = 2$, $df_{depths} = 4$, $p = 0.17$).

Heatwave treatments significantly changed the depth-averaged bioturbated area (Kruskal–Wallis test, $\chi^2 = 7.2884$, $df = 2$, $p = 0.03$). Further post hoc analysis indicated that the 6-d cycle heatwaves significantly decreased the depth-averaged bioturbated area compared to that under 3-d cycle heatwaves (*see* Fig. 4a, Wilcoxon rank sum test, IL_6–FS_3, effect size $r = 0.63$, $N = 17$, $p = 0.02$).

In summary, the 6-d cycle heatwaves (IL_6,) imposed higher mortality than the 3-d cycle heatwaves (FS_3) (Fig. SA2) and decreased cockles' bioturbation ability (Fig. 3), thus significantly reducing the size of the depth-averaged bioturbation area (Fig. 4a). FS_3 heatwaves boosted

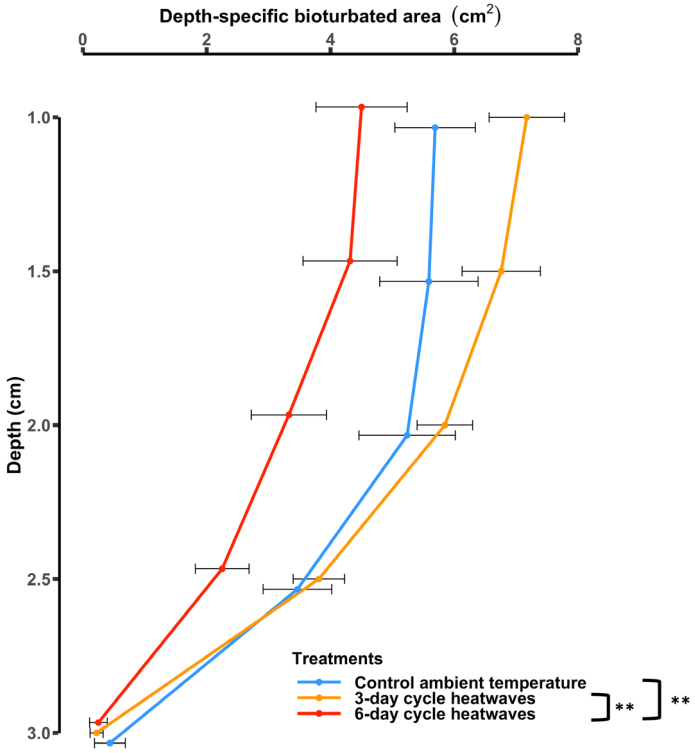

Fig. 3. The depth-specific bioturbated area ($S_{bioturb\text{-}depth}$, cm^2) for contrasting heatwave treatments. The bioturbation areas were calculated using luminophore pixel counting data. Each point represents 8–10 data recordings in the plot depending on the number of successfully processed PVC pots. Only 1.0–3.0 cm profiles were displayed since most of the bioturbation process happened within this range. The top 1 cm layer results were discarded after slicing due to pervasive edge effects. Each data point represents the mean values of the measured replicates. The error bars represent the standard errors between replicate PVC pots at each depth. The significant level of $p < 0.01$ was indicated by "**" in the figure legend.

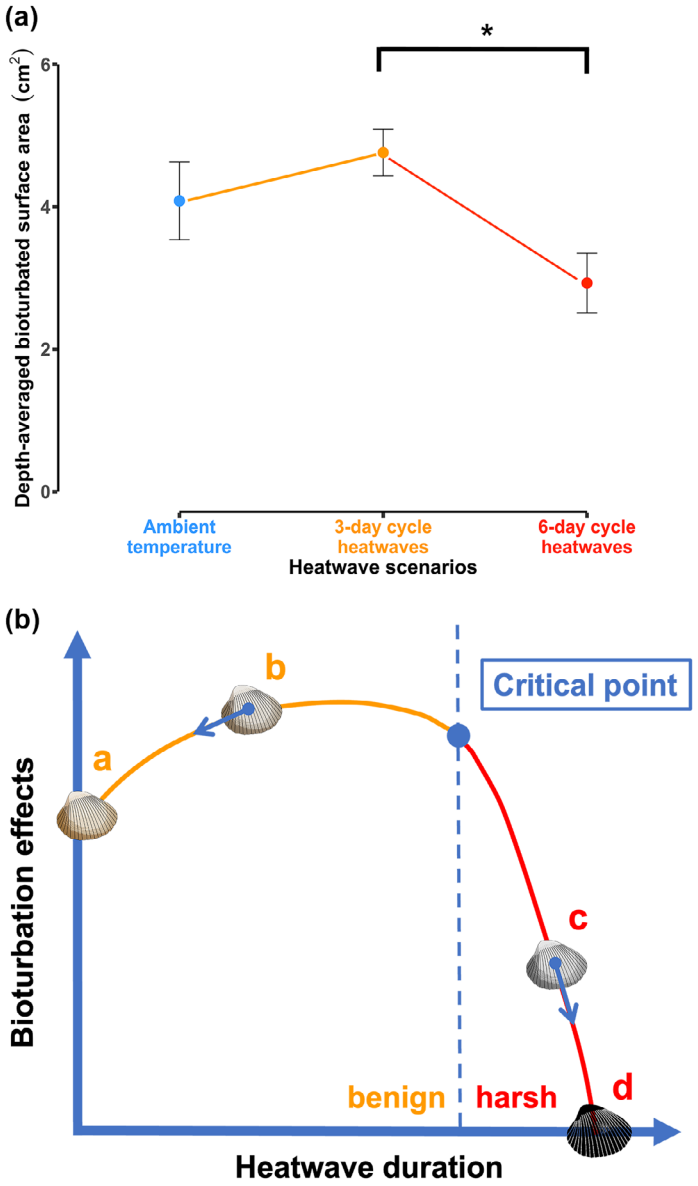

Fig. 4. Diagrams showing how the heatwave duration may determine bioturbation effects. (**a**) Experiment data that summarizes heatwave effects on the depth-averaged bioturbated area. Each data point represents the mean values of the measured replicates. The 3-d cycle heatwaves result in more bioturbation areas than those under ambient temperatures. The 6-d cycle heatwaves decrease depth-averaged bioturbated areas compared with ambient temperatures. Each data point represents the mean values of the measured replicates. The error bars represent the standard errors between replicate PVC pots. The significant level of $p < 0.05$ was indicated by "*" in the figure. (**b**) A conceptual figure showing how cockles' behavioral response can determine the bioturbation under heatwaves. The *x*-axis indicates the duration of heatwaves. The *y*-axis shows the bioturbation intensity in tidal flat sediment. When the heatwave duration does not pass the critical point of bioturbators' thermal tolerance thresholds, the bioturbation can be enhanced due to more movements (status "a" to "b"). After the heatwaves, bioturbators' condition may still recover (as indicated by the blue arrow on "b"). When the heatwave duration lasts too long, bioturbators' health conditions are reduced, leading to reduced bioturbation effects (status "a" to "c"). In the worst case, the bioturbator may no longer be able to recover (as indicated by the blue arrow on "c"), resulting in mass mortality (status "d").

vertical (Fig. 2b) and horizontal (Fig. 3) bioturbation activity, yet the total bioturbated areas did not show a significant difference with those under ambient temperature after 3 d of sediment reworking (Fig. 4a).

Discussion

Studying bioturbation under heatwaves is essential to understand the effects of global warming on the tidal flat sedimentary environment, as bioturbation is known to affect both the sediment mixing and the erodibility of tidal flats. In the present study, we show for the first time that bioturbation effects under global warming strongly depend on the frequency and duration of the heatwaves. That is, repeated short heatwaves can increase bioturbation activity while not causing much mortality. In contrast, the less frequent long-duration heatwaves decrease the overall bioturbation activity as it increases bioturbators' mortality, thereby causing less sediment mixing. Predicting climate-change effects on tidal flat functioning requires insights into the frequency and duration of future heatwaves and in-depth studies on the behavioral responses and mortality consequences of key bioturbating species, as demonstrated in the current study.

Thermal tolerance of organisms in the face of climate change

In our experiment, cockles that suffered from 3-d repetitions of heating treatments showed more vertical movement than those under ambient temperatures. This response can be seen as a strategy in which bioturbators adjust their burial depth and use the sediment as a thermal refuge during the heatwave (Payette and McGaw 2003; Munguia et al. 2017). Other bivalve species also adapt their burial depth to elevated temperatures. For example, a mesocosm experiment showed that *Ruditapes decussatus* burrowed deeper into the sediment under simulated heat stress of 29°C to 8 cm depth (Domínguez et al. 2021). Compared with *C. edule*, *R. decussatus* typically buries deeper into the sediment, potentially down to 20 cm (Macho et al. 2016). Therefore, we summarize the response strategies by which benthic organisms cope with extreme temperatures with the following two strategies: (1) either employing more horizontal movements to search for locations with less stressful temperature conditions; or (2) burrowing deeper to use deep layers of the sediment as a shelter to escape the extreme heat stress. The trade-offs between these two strategies will likely depend on a species' physiological limitations and energy consumption. For example, the maximal burrowing depth of bioturbating bivalves is mainly limited by their siphon size (i.e., physiological limitation) (Zwarts and Wanink 1989). However, higher filtration costs due to enhanced movements will typically increase the energy consumption of these bivalves (Sobral and Widdows 2000).

These strategies can be regarded as regulatory behaviors that are stimulated by the environmental conditions of microhabitats. Microhabitats are usually local habitats with less harsh environmental conditions than those at larger spatial scales. Many intertidal ectotherms have developed a range of behavioral strategies to search for suitable microhabitats and adapt to temperature variations (Williams 1984; Muñoz et al. 2005). In cooler environments, most freshwater insect larvae avoid freezing by actively staying in the water body that will not freeze; lizards will shuttle between the sun and shade to maintain their body temperature in an optimal range (Lencioni 2004; Diaz and Cabezas-Diaz 2004). In a warmer environment, snails may actively search for sheltered microhabitats on rocky shores to escape direct sunlight and stabilize their body temperatures during daytime emersion; capitellids may burrow deeper to escape warm temperatures that exist in natural soft sediments (Tsubokura et al. 1997; Lardies et al. 2001). The movement behaviors demonstrated by cockles in our experiments could be considered an example of the wide range of thermoregulatory movement responses commonly practiced by ectotherms.

Tidal flat invertebrates may cope temporarily with thermal stress through thermoregulatory behaviors such as burrowing. However, when the thermal stress (e.g., magnitude, duration, etc.) surpasses critical thresholds, these response strategies may fail and lead to severe physiological stress or even mass mortality (Fig. 4b). The findings by Deldicq et al. (2021) also support the conceptual summary shown in Fig. 4b, in that foraminifera reduced their activity by up to 80% under high-temperature regimes (i.e., 36°C) and the photosynthetic activity of their sequestered chloroplasts significantly decreased. When the heatwave duration is long enough to create mass mortality (50% death rate in this experiment), organisms cannot escape from the continuous accumulation of heat stress via different behavioral strategies. The resulting mass mortality can potentially cause large-scale species distribution shifts (Fiori and Cazzaniga 1999; Wernberg et al. 2013; Pairaud et al. 2014). Due to the mass mortality of adult individuals, the age structure of native species tends to be younger in the following year (Magalhães et al. 2016; Beukema and Dekker 2020). This implies that if the duration of heatwaves strongly increases under climate-change scenarios, there will not be enough adults to produce larvae. As a result, native species with poor temperature tolerance will not persist, thereby giving up their niche to more heat-tolerant invasive species (Molnar et al. 2008). Both native species depletion and invasive species replacement can result in functioning shifts of the whole tidal flat ecosystems.

Implications for bioturbation in tidal flat ecosystems

Our experiment provides novel insights into the effects of heatwaves on tidal flats by demonstrating that the temporal scale of heatwaves is a key factor in driving the overall bioturbation outcome (Fig. 4b). High temperature promotes bioturbation rates via increased metabolism (Ouellette et al. 2004; Pörtner and Farrell 2008; Cozzoli et al. 2019). In this experiment, repeated short-duration heatwaves increased cockles' burrowing activities, as shown in their daily burrowing depth change. Studies have shown that bioturbation activities result in higher erodibility dependent on sediment type and suspended particle content (Willows et al. 1998; Li et al. 2017). Thus, more erosion can be expected under short-duration heatwaves. Moreover, bioturbating activities promote sediment mixing and chemical resource exchange (Mermillod-Blondin and Rosenberg 2006; Sturdivant and Shimizu 2017). To our surprise, the luminophore tests yielded a similar bioturbation effect between the control and FS_3 heatwaves. This similarity might be due to the relatively long 3-d action duration before slicing and the limited volume of the PVC pots. Cockles living in the small PVC pots thus had sufficient time to disturb most of the sediments. Nevertheless, previous studies indicated that enhanced burrowing activities under short-duration heatwaves potentially resulted in a deeper oxygen penetration (Weissberger et al. 2009; Sturdivant et al. 2012), which will further change the bottom chemical conditions for microbial communities and other organisms (Jørgensen and Des Marais 1990).

However, temperature regimes beyond physiological thresholds can impede bioturbators' activities to reduce the animals' energy consumption (Pörtner 2001; Wu et al. 2017; da Silva Vianna et al. 2020). For example, the mudflat foraminifera *Haynesina germanica* can contribute most to sediment reworking under moderate temperatures between 6°C and 30°C, yet significantly reduce activities by 75% under extremely high temperatures (i.e., 32–36°C, Deldicq et al. 2021). The opportunistic deposit-feeding polychaete *Capitella* sp. burrowed significantly deeper at 21°C than at 15°C; however, they suffer from mortality at 32°C (Przeslawski et al. 2009). Similar responses were observed in our experiment: the biodisturbed area under the IL_6 heatwave was significantly lower than the ambient control temperature, though cockles' burrowing depth varied during the heatwaves.

Heatwaves are usually fragmented by mild temperature periods, during which the organisms may recover from the thermal stress (Woodin et al. 2013; Pansch et al. 2018). The tolerance landscape theory by Rezende et al. (2014) states that species-specific tolerance thresholds are determined by the stress event's intensity and duration. In addition, our study revealed the importance of the heatwave temporal dynamics in determining bioturbators' thermal tolerance thresholds. Present findings are conceptualized in a generic schematization as Fig. 4b. Although our experiment settings indicate significant effects of heatwave duration and frequency in soft sediments, the current conceptualizations can be enlarged to other species and broader habitats. For example, the study by Seuront et al. (2019) showed that the mussel *M. edulis* living on rocky shores suffered a 100% mortality when exposed only

once to 41°C for 6 h, while they also suffered a 100% mortality when exposed five times to 32°C for 6 h. Moreover, another rocky-shore species *Littorina littorea* also showed a similar response pattern to heatwaves that the temperature at which its heat coma occurred declined significantly with repeated daily exposures (Clarke et al. 2000). These results together indicate that the temporal dynamics of the heatwaves are one of the determining factors for the species sustainability in tidal flat ecosystems, especially under the current global change scenarios featured by increasing frequency and duration of heatwaves.

The present novel findings show that it is the combination of heatwave frequency and duration that determines the outcome of ecosystem functioning like bioturbation. We thus call for action to gain a broader knowledge based on how key bioturbating species respond to the interaction between heatwave frequency and duration, and its meaning for multiple other key species inhabiting tidal flats. This is the only way toward quantifying in detail the conceptualized relationship (Fig. 4b) at the community level.

Data availability statement

Code and data to replicate analyses are summarized by the order of figures, and they are available at: https://dataportal.nioz.nl/doi/10.25850/nioz/7b.b.7d.

References

Anestis, A., A. Lazou, H. O. Pörtner, and B. Michaelidis. 2007. Behavioral, metabolic, and molecular stress responses of marine bivalve *Mytilus galloprovincialis* during long-term acclimation at increasing ambient temperature. Am. J. Physiol. Regul. Integr. Comp. Physiol. **293**: R911–R921. doi:10.1152/ajpregu.00124.2007

Auffrey, L., S. Robinson, and M. Barbeau. 2004. Effect of green macroalgal mats on burial depth of soft-shelled clams *Mya arenaria*. Mar. Ecol. Prog. Ser. **278**: 193–203. doi:10.3354/meps278193

Beukema, J. J., and R. Dekker. 2020. Winters not too cold, summers not too warm: Long-term effects of climate change on the dynamics of a dominant species in the Wadden Sea: The cockle *Cerastoderma edule* L. Mar. Biol. **167**: 44. doi:10.1007/s00227-020-3659-1

Borsje, B. W., T. J. Bouma, M. Rabaut, P. M. J. Herman, and S. J. M. H. Hulscher. 2014. Formation and erosion of biogeomorphological structures: A model study on the tube-building polychaete *Lanice conchilega*. Limnol. Oceanogr. **59**: 1297–1309. doi:10.4319/lo.2014.59.4.1297

Bouchet, V. M. P., J.-P. Debenay, P.-G. Sauriau, J. Radford-Knoery, and P. Soletchnik. 2007. Effects of short-term environmental disturbances on living benthic foraminifera during the Pacific oyster summer mortality in the Marennes-Oléron Bay (France). Mar. Environ. Res. **64**: 358–383. doi:10.1016/j.marenvres.2007.02.007

Bouma, T. J., and others. 2016. Short-term mudflat dynamics drive long-term cyclic salt marsh dynamics. Limnol. Oceanogr. **61**: 2261–2275. doi:10.1002/lno.10374

Braeckman, U., P. Provoost, B. Gribsholt, D. Van Gansbeke, J. Middelburg, K. Soetaert, M. Vincx, and J. Vanaverbeke. 2010. Role of macrofauna functional traits and density in biogeochemical fluxes and bioturbation. Mar. Ecol. Prog. Ser. **399**: 173–186. doi:10.3354/meps08336

Clarke, A. P., P. J. Mill, and J. Grahame. 2000. The nature of heat coma in *Littorina littorea* (Mollusca: Gastropoda). Mar. Biol. **137**: 447–451. doi:10.1007/s002270000367

Coma, R., M. Ribes, E. Serrano, E. Jimenez, J. Salat, and J. Pascual. 2009. Global warming-enhanced stratification and mass mortality events in the Mediterranean. Proc. Natl. Acad. Sci. USA **106**: 6176–6181. doi:10.1073/pnas.0805801106

Cozzoli, F., V. Gjoni, M. Del Pasqua, Z. Hu, T. Ysebaert, P. M. J. Herman, and T. J. Bouma. 2019. A process based model of cohesive sediment resuspension under bioturbators' influence. Sci. Total Environ. **670**: 18–30. doi:10.1016/j.scitotenv.2019.03.085

Cozzoli, F., and others. 2020. Biological and physical drivers of bio-mediated sediment resuspension: A flume study on *Cerastoderma edule*. Estuar. Coast. Shelf Sci. **241**: 106824. doi:10.1016/j.ecss.2020.106824

Cozzoli, F., and others. 2021. Modelling spatial and temporal patterns in bioturbator effects on sediment resuspension: A biophysical metabolic approach. Sci. Total Environ. **792**: 148215. doi:10.1016/j.scitotenv.2021.148215

da Silva Vianna, B., C. A. Miyai, A. Augusto, and T. M. Costa. 2020. Effects of temperature increase on the physiology and behavior of fiddler crabs. Physiol. Behav. **215**: 112765. doi:10.1016/j.physbeh.2019.112765

Dairain, A., O. Maire, G. Meynard, A. Richard, T. Rodolfo-Damiano, and F. Orvain. 2020. Sediment stability: Can we disentangle the effect of bioturbating species on sediment erodibility from their impact on sediment roughness? Mar. Environ. Res. **162**: 105147. doi:10.1016/j.marenvres.2020.105147

Darwin, C. 1881. The formation of vegetable mould through the action of worms with observation of their habits. John Murray.

Deldicq, N., D. Langlet, C. Delaeter, G. Beaugrand, L. Seuront, and V. M. P. Bouchet. 2021. Effects of temperature on the behaviour and metabolism of an intertidal foraminifera and consequences for benthic ecosystem functioning. Sci. Rep. **11**: 4013. doi:10.1038/s41598-021-83311-z

Diaz, J. A., and S. Cabezas-Diaz. 2004. Seasonal variation in the contribution of different behavioural mechanisms to lizard thermoregulation. Functional Ecology, **18**(6): 867–875. https://doi.org/10.1111/j.0269-8463.2004.00916.x

Domínguez, R., C. Olabarria, S. A. Woodin, D. S. Wethey, L. G. Peteiro, G. Macho, and E. Vázquez. 2021. Contrasting responsiveness of four ecologically and economically important bivalves to simulated heat waves. Mar. Environ. Res. **164**: 105229. doi:10.1016/j.marenvres.2020.105229

Donohue, I., and others. 2016. Navigating the complexity of ecological stability. Ecol. Lett. **19**: 1172–1185. doi:10.1111/ele.12648

Fiori, S. M., and N. J. Cazzaniga. 1999. Mass mortality of the yellow clam, *Mesodesma mactroides* (Bivalvia: Mactracea) in Monte Hermoso beach, Argentina. Biol. Conserv. **89**: 305–309. doi:10.1016/S0006-3207(98)00151-7

Gauzens, B., B. C. Rall, V. Mendonça, C. Vinagre, and U. Brose. 2020. Biodiversity of intertidal food webs in response to warming across latitudes. Nat. Clim. Change **10**: 264–269. doi:10.1038/s41558-020-0698-z

Goulletquer, P., P. Soletchnik, O. Le Moine, D. Razet, P. Geairon, and N. Faury. 1998. Summer mortality of the Pacific cupped oyster *Crassostrea gigas* in the bay of Marennes-Oléron (France). CIEM Conseil International pour l'Exploration de la Mer.

Hedman, J. E., J. S. Gunnarsson, G. Samuelsson, and F. Gilbert. 2011. Particle reworking and solute transport by the sediment-living polychaetes *Marenzelleria neglecta* and *Hediste diversicolor*. J. Exp. Mar. Biol. Ecol. **407**: 294–301. doi:10.1016/j.jembe.2011.06.026

Holbrook, N. J., and others. 2019. A global assessment of marine heatwaves and their drivers. Nat. Commun. **10**: 2624. doi:10.1038/s41467-019-10206-z

Johnson, R. G. 1965. Temperature variation in the infaunal environment of a sand flat. Limnol. Oceanogr. **10**: 114–120. doi:10.4319/lo.1965.10.1.0114

Jones, C. G., J. H. Lawton, and M. Shachak. 1997. Positive and negative effects of organisms as physical ecosystem engineers. Ecology **78**: 1946–1957. doi:10.1890/0012-9658(1997)078[1946:PANEOO]2.0.CO;2

Jørgensen, B. B., and D. J. Des Marais. 1990. The diffusive boundary layer of sediments: Oxygen microgradients over a microbial mat. Limnol. Oceanogr. **35**: 1343–1355. doi:10.4319/lo.1990.35.6.1343

Kristensen, E., G. Penha-Lopes, M. Delefosse, T. Valdemarsen, C. Quintana, and G. Banta. 2012. What is bioturbation? The need for a precise definition for fauna in aquatic sciences. Mar. Ecol. Prog. Ser. **446**: 285–302. doi:10.3354/meps09506

Lardies, M. A., E. Clasing, J. M. Navarro, and R. A. Stead. 2001. Effects of environmental variables on burial depth of two infaunal bivalves inhabiting a tidal flat in southern Chile. J. Mar. Biol. Assoc. UK **81**: 809–816. doi:10.1017/S0025315401004635

Laufkötter, C., J. Zscheischler, and T. L. Frölicher. 2020. High-impact marine heatwaves attributable to human-induced global warming. Science **369**: 1621–1625. doi:10.1126/science.aba0690

Le Hir, P., Y. Monbet, and F. Orvain. 2007. Sediment erodability in sediment transport modelling: Can we account for biota effects? Cont. Shelf Res. **27**: 1116–1142. doi:10.1016/j.csr.2005.11.016

Lencioni, V. 2004. Survival strategies of freshwater insects in cold environments. Journal of Limnology, **63**(1s): 45. https://doi.org/10.4081/jlimnol.2004.s1.45

Li, B., F. Cozzoli, L. M. Soissons, T. J. Bouma, and L. Chen. 2017. Effects of bioturbation on the erodibility of cohesive versus non-cohesive sediments along a current-velocity gradient: A case study on cockles. J. Exp. Mar. Biol. Ecol. **496**: 84–90. doi:10.1016/j.jembe.2017.08.002

Li, Y., M. Zheng, J. Lin, S. Zhou, T. Sun, and N. Xu. 2019. Darkness and low nighttime temperature modulate the growth and photosynthetic performance of *Ulva prolifera* under lower salinity. Mar. Pollut. Bull. **146**: 85–91. doi:10.1016/j.marpolbul.2019.05.058

Macho, G., S. A. Woodin, D. S. Wethey, and E. Vázquez. 2016. Impacts of sublethal and lethal high temperatures on clams exploited in European fisheries. J. Shellfish. Res. **35**: 405–419. doi:10.2983/035.035.0215

Magalhães, L., R. Freitas, and X. de Montaudouin. 2016. Cockle population dynamics: Recruitment predicts adult biomass, not the inverse. Mar. Biol. **163**: 16. doi:10.1007/s00227-015-2809-3

Mermillod-Blondin, F., and R. Rosenberg. 2006. Ecosystem engineering: The impact of bioturbation on biogeochemical processes in marine and freshwater benthic habitats. Aquat. Sci. **68**: 434–442. doi:10.1007/s00027-006-0858-x

Meysman, F., J. Middelburg, and C. Heip. 2006. Bioturbation: A fresh look at Darwin's last idea. Trends Ecol. Evol. **21**: 688–695. doi:10.1016/j.tree.2006.08.002

Molnar, J. L., R. L. Gamboa, C. Revenga, and M. D. Spalding. 2008. Assessing the global threat of invasive species to marine biodiversity. Front. Ecol. Environ. **6**: 485–492. doi:10.1890/070064

Montserrat, F., C. Van Colen, P. Provoost, M. Milla, M. Ponti, K. Van den Meersche, T. Ysebaert, and P. M. J. Herman. 2009. Sediment segregation by biodiffusing bivalves. Estuar. Coast. Shelf Sci. **83**: 379–391. doi:10.1016/j.ecss.2009.04.010

Munguia, P., P. R. Y. Backwell, and M. Z. Darnell. 2017. Thermal constraints on microhabitat selection and mating opportunities. Anim. Behav. **123**: 259–265. doi:10.1016/j.anbehav.2016.11.004

Muñoz, J. L. P., G. Randall Finke, P. A. Camus, and F. Bozinovic. 2005. Thermoregulatory behavior, heat gain and thermal tolerance in the periwinkle *Echinolittorina peruviana* in central Chile. Comp. Biochem. Physiol. A Mol. Integr. Physiol. **142**: 92–98. doi:10.1016/j.cbpa.2005.08.002

Murphy, E. A. K., and M. A. Reidenbach. 2016. Oxygen transport in periodically ventilated polychaete burrows. Mar. Biol. **163**: 208. doi:10.1007/s00227-016-2983-y

Murray, N. J., and others. 2019. The global distribution and trajectory of tidal flats. Nature **565**: 222–225. doi:10.1038/s41586-018-0805-8

Oliver, E. C. J., and others. 2018. Longer and more frequent marine heatwaves over the past century. Nat. Commun. **9**: 1324. doi:10.1038/s41467-018-03732-9

Ouellette, D., G. Desrosiers, J. Gagne, F. Gilbert, J. Poggiale, P. Blier, and G. Stora. 2004. Effects of temperature on in vitro

sediment reworking processes by a gallery biodiffusor, the polychaete *Neanthes virens*. Mar. Ecol. Prog. Ser. **266**: 185–193. doi:10.3354/meps266185

Pairaud, I. L., N. Bensoussan, P. Garreau, V. Faure, and J. Garrabou. 2014. Impacts of climate change on coastal benthic ecosystems: Assessing the current risk of mortality outbreaks associated with thermal stress in NW Mediterranean coastal areas. Ocean Dyn. **64**: 103–115. doi:10.1007/s10236-013-0661-x

Pansch, C., and others. 2018. Heat waves and their significance for a temperate benthic community: A near-natural experimental approach. Glob. Change Biol. **24**: 4357–4367. doi:10.1111/gcb.14282

Payette, A. L., and I. J. McGaw. 2003. Thermoregulatory behavior of the crayfish *Procambarus clarki* in a burrow environment. Comp. Biochem. Physiol. A Mol. Integr. Physiol. **136**: 539–556. doi:10.1016/S1095-6433(03)00203-4

Perkins-Kirkpatrick, S. E., E. M. Fischer, O. Angélil, and P. B. Gibson. 2017. The influence of internal climate variability on heatwave frequency trends. Environ. Res. Lett. **12**: 044005. doi:10.1088/1748-9326/aa63fe

Pörtner, H.-O. 2001. Climate change and temperature-dependent biogeography: Oxygen limitation of thermal tolerance in animals. Naturwissenschaften **88**: 137–146. doi:10.1007/s001140100216

Pörtner, H. O., and A. P. Farrell. 2008. Physiology and climate change. Science **322**: 690–692. doi:10.1126/science.1163156

Przeslawski, R., Q. Zhu, and R. Aller. 2009. Effects of abiotic stressors on infaunal burrowing and associated sediment characteristics. Mar. Ecol. Prog. Ser. **392**: 33–42. doi:10.3354/meps08221

R Core Team. 2021. R: A language and environment for statistical computing. R Foundation for Statistical Computing.

Rezende, E. L., L. E. Castañeda, and M. Santos. 2014. Tolerance landscapes in thermal ecology. Funct. Ecol. **28**: 799–809. doi:10.1111/1365-2435.12268

Rivetti, I., S. Fraschetti, P. Lionello, E. Zambianchi, and F. Boero. 2014. Global warming and mass mortalities of benthic invertebrates in the Mediterranean Sea. PLoS ONE **9**: e115655. doi:10.1371/journal.pone.0115655

Seuront, L., K. R. Nicastro, G. I. Zardi, and E. Goberville. 2019. Decreased thermal tolerance under recurrent heat stress conditions explains summer mass mortality of the blue mussel *Mytilus edulis*. Sci. Rep. **9**: 17498. doi:10.1038/s41598-019-53580-w

Shi, B., and others. 2021. Effect of typhoon-induced intertidal-flat erosion on dominant macrobenthic species (*Meretrix meretrix*). Limnol. Oceanogr. **66**: 4197–4209. doi:10.1002/lno.11953

Sobral, P., and J. Widdows. 2000. Effects of increasing current velocity, turbidity and particle-size selection on the feeding activity and scope for growth of *Ruditapes decussatus* from Ria Formosa, southern Portugal. J. Exp. Mar. Biol. Ecol. **245**: 111–125. doi:10.1016/S0022-0981(99)00154-9

Sturdivant, S. K., and M. S. Shimizu. 2017. In situ organism-sediment interactions: Bioturbation and biogeochemistry in a highly depositional estuary. PLoS ONE **12**: e0187800. doi:10.1371/journal.pone.0187800

Sturdivant, S. K., R. J. Díaz, and G. R. Cutter. 2012. Bioturbation in a declining oxygen environment, in situ observations from Wormcam. PLoS ONE **7**: e34539. doi:10.1371/journal.pone.0034539

Teal, L., M. Bulling, E. Parker, and M. Solan. 2008. Global patterns of bioturbation intensity and mixed depth of marine soft sediments. Aquat. Biol. **2**: 207–218. doi:10.3354/ab00052

Tsubokura, T., S. Goshima, and S. Nakao. 1997. Seasonal horizontal and vertical distribution patterns of the supralittoral amphipod *Trinorchestia trinitatis* in relation to environmental variables. J. Crustac. Biol. **17**: 674–686. doi:10.1163/193724097X00107

van der Wal, D., G. I. Lambert, T. Ysebaert, Y. M. G. Plancke, and P. M. J. Herman. 2017. Hydrodynamic conditioning of diversity and functional traits in subtidal estuarine macrozoobenthic communities. Estuar. Coast. Shelf Sci. **197**: 80–92. doi:10.1016/j.ecss.2017.08.012

Vinagre, C., I. Leal, V. Mendonça, D. Madeira, L. Narciso, M. S. Diniz, and A. A. V. Flores. 2016. Vulnerability to climate warming and acclimation capacity of tropical and temperate coastal organisms. Ecol. Indic. **62**: 317–327. doi:10.1016/j.ecolind.2015.11.010

Weissberger, E. J., L. L. Coiro, and E. W. Davey. 2009. Effects of hypoxia on animal burrow construction and consequent effects on sediment redox profiles. J. Exp. Mar. Biol. Ecol. **371**: 60–67. doi:10.1016/j.jembe.2009.01.005

Wernberg, T., D. A. Smale, F. Tuya, M. S. Thomsen, T. J. Langlois, T. de Bettignies, S. Bennett, and C. S. Rousseaux. 2013. An extreme climatic event alters marine ecosystem structure in a global biodiversity hotspot. Nat. Clim. Change **3**: 78–82. doi:10.1038/nclimate1627

Widdows, J., S. Brown, M. D. Brinsley, P. N. Salkeld, and M. Elliott. 2000. Temporal changes in intertidal sediment erodability: Influence of biological and climatic factors. Cont. Shelf Res. **20**: 1275–1289. doi:10.1016/S0278-4343(00)00023-6

Widdows, J., and M. Brinsley. 2002. Impact of biotic and abiotic processes on sediment dynamics and the consequences to the structure and functioning of the intertidal zone. J. Sea Res. **48**: 143–156. doi:10.1016/S1385-1101(02)00148-X

Wiesebron, L. E., N. Steiner, C. Morys, T. Ysebaert, and T. J. Bouma. 2021. Sediment bulk density effects on benthic macrofauna burrowing and bioturbation behavior. Front. Mar. Sci. **8**: 707785. doi:10.3389/fmars.2021.707785

Williams, J. B. 1984. Respiratory changes in the euryhaline clam, *Mulinialateralis* (Say), over a range of temperature and salinity combinations. J. Exp. Mar. Biol. Ecol. **81**: 269–280. doi:10.1016/0022-0981(84)90146-1

Willows, R. I., J. Widdows, and R. G. Wood. 1998. Influence of an infaunal bivalve on the erosion of an intertidal cohesive sediment: A flume and modeling study. Limnol. Oceanogr. **43**: 1332–1343. doi:10.4319/lo.1998.43.6.1332

Woodin, S. A., T. J. Hilbish, B. Helmuth, S. J. Jones, and D. S. Wethey. 2013. Climate change, species distribution models, and physiological performance metrics: Predicting when biogeographic models are likely to fail. Ecol. Evol. **3**: 3334–3346. doi:10.1002/ece3.680

Wrede, A., J. Beermann, J. Dannheim, L. Gutow, and T. Brey. 2018. Organism functional traits and ecosystem supporting services—A novel approach to predict bioirrigation. Ecol. Indic. **91**: 737–743. doi:10.1016/j.ecolind.2018.04.026

Wright, J. P., and C. G. Jones. 2006. The concept of organisms as ecosystem engineers ten years on: Progress, limitations, and challenges. Bioscience **56**: 203. doi:10.1641/0006-3568(2006)056[0203:TCOOAE]2.0.CO;2

Wu, F., and others. 2017. Effects of seawater pH and temperature on foraging behavior of the Japanese stone crab *Charybdis japonica*. Mar. Pollut. Bull. **120**: 99–108. doi:10.1016/j.marpolbul.2017.04.053

Zhou, Z., T. J. Bouma, G. S. Fivash, T. Ysebaert, L. Van IJzerloo, J. van Dalen, B. van Dam, and B. Walles. 2022. Thermal stress affects bioturbators' burrowing behavior: A mesocosm experiment on common cockles (*Cerastoderma edule*). Sci. Total Environ. **824**: 153621. doi:10.1016/j.scitotenv.2022.153621

Zwarts, L., and J. Wanink. 1989. Siphon size and burying depth in deposit- and suspension-feeding benthic bivalves. Mar. Biol. **100**: 227–240. doi:10.1007/BF00391963

Acknowledgments

We gratefully thank the following colleagues: Arne den Toonder for assistance with equipment and mesocosm realization; Pieter van Rijswijk for his technical expertise in the respiration measurements; Jim van Belzen for suggestions on data analysis and visualization; Jaco de Smith for comments on manuscript writing; Simon Hof for helping build up the mesocosms; Victor Malagon Santos for advice on the statistics of heatwave events. This project was sponsored and funded by Extreme droughts and the Dutch water sector: impacts and adaptation (Grant ID: NWA.1418.20.04), and was financed by "Coping with deltas in transition" within the Programme of Strategic Scientific Alliances between China and the Netherlands (PSA, Grant ID: PSA-SA-E-02). The first author (Z.Z.) was supported by the China Scholarship Council (CSC, Grant ID: 201804910683).

Conflict of Interest

None declared.

Submitted 16 March 2022
Revised 27 September 2022
Accepted 08 February 2023

Associate editor: Josef Daniel Ackerman